Buckling analysis of carbon nanotubes modeled using nonlocal continuum theories

Devesh Kumar, Christian Heinrich, and Anthony M. Waas[a)]
Department of Aerospace Engineering, University of Michigan, Ann Arbor, MI 48109, USA

(Received 2 October 2007; accepted 25 January 2008; published online 9 April 2008)

In this paper, the buckling of carbon nanotubes, modeled as nonlocal one dimensional continua within the framework of Euler–Bernoulli beams, is considered. Both a stress gradient and a strain gradient approach are considered and a variational approach is adopted to obtain the variationally consistent boundary conditions. The dependence of the buckling load on the nonlocal parameter has been determined using the boundary conditions obtained from the variational analysis. Results indicate significant dependence of nonlocal parameter on buckling load for particular types of boundary conditions. These findings are important in mechanical design considerations of devices that use carbon nanotubes. © *2008 American Institute of Physics*. [DOI: 10.1063/1.2901201]

I. INTRODUCTION

Since the discovery of carbon nanotubes (CNTs), in 1991,[1] a considerable amount of research has been conducted to evaluate the mechanical, thermal, electrical, and electromagnetic properties of CNTs and CNT reinforced nanocomposites. CNTs are reported to have a very high elastic modulus (1 TPa) and an ultimate strength that is 100 times that of steel.[2] They are thermally stable up to 2800 °C in vacuum, with a thermal conductivity which is twice as large as diamond, and having an electric-current-carrying capacity about 1000 times greater than copper wire.[2] These exceptional properties make them ideal candidates for a variety of applications.[3] Probes that exploit length scales down to the molecular level for biological and chemical applications are shown in Figs. 1 and 2.

In many nanoscale applications, CNTs by themselves or embedded within other substrates are subjected to axial compressive loads and as a consequence their buckling behavior has received attention in the past.[6,7] Associated with analyzing the buckling response is an examination of the various ways in which the CNTs can be modeled for mechanical purposes.

Molecular dynamics (MD) simulations are the most common method in examining CNT behavior.[8,9] The atoms are modeled as solid point masses with a force potential that captures interactions between them. Newton's laws of motion are applied to each atom and a system of coupled differential equations is solved to obtain the time evolution of the motion of the system. Due to the computational restrictions such models usually use a cut off radius that limits the domain of interaction between atoms. This limits the amount of interactions between atoms far away from each other and leaves room for discussion as to what happens if the total interaction between all atoms is considered. Yakobson *et al.*[10] have discussed the response of CNTs subjected to high strains using MD. It was found that CNTs can sustain very high strains without the atomic bond breaking. Simulations showed that dilatation of up to 40% does not result in a damage of the graphite arrangement. This is an unexpected behavior for a brittle material like graphite. Zhang *et al.*[7] used MD to determine the influence of the chiral angle on the buckling behavior of single walled carbon nanotubes (SWCNTs). They suggested that SWCNTs have similar buckling modes (independent of chirality) except for the zigzag SWCNT and that the buckling strains decrease with increasing chiral angles.

Noting the significant computational costs of MD simulations, other approaches have emerged for the modeling of CNTs. These include the use of structural mechanics models of the CNT structure (Li *et al.*[11]). A CNT is modeled as a framelike structure. Since the forces between the atoms not only depend on the stretching but also on the bond angle, bending dihedral angle torsion, improper (out-of-plane) torsion, and van der Waals interaction, a relationship between these forces and the usual terms of the beam energy has been established. While the method is computationally efficient, it

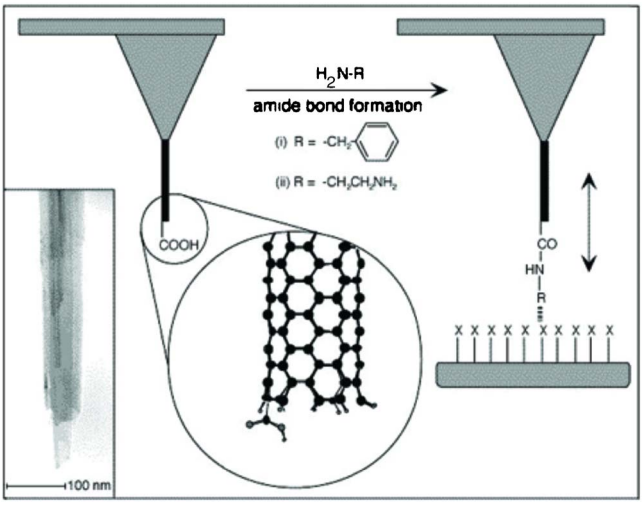

FIG. 1. (Color online) Diagram illustrating the modification of a nanotube tips by coupling in amine to a pendant carboxylic group and application of this probe to sense specific interaction with functional groups (*X*) of a substrate (Ref. 4).

[a)]Electronic mail: dcw@umich.edu. URL: http://www.engin.umich.edu/dept/aero/people/faculty/waas/

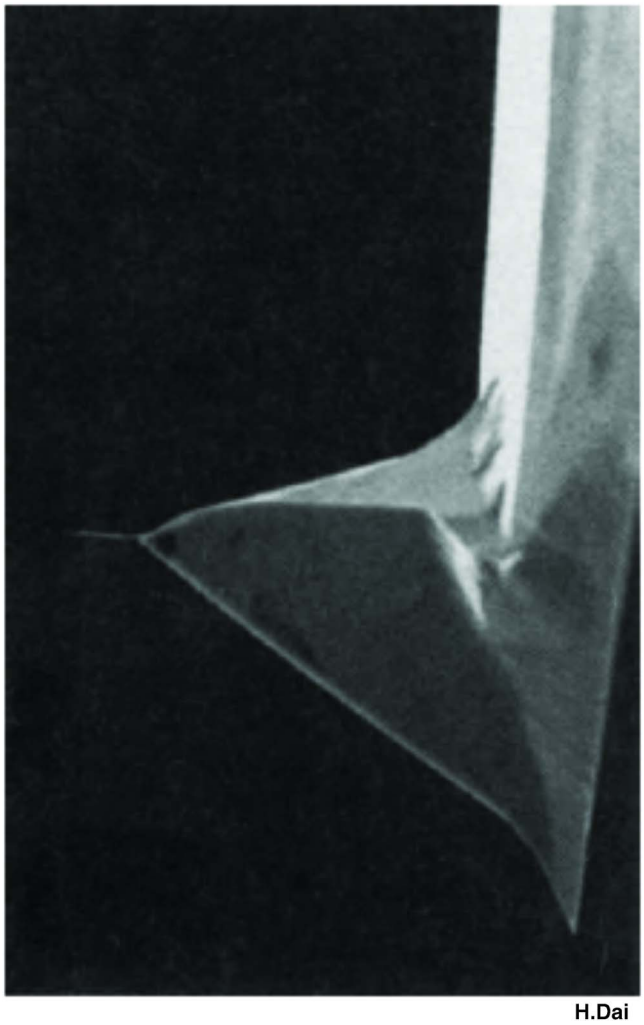

FIG. 2. (Color online) CNT struck on the end of a conventional silicon probe used in scanning force microscopy (Ref. 5).

relies on proper translations from the atomic interactions to the different beam stiffnesses that appear in defining the beam's strain energy. The results obtained show that Young's modulus increases with tube diameter and that CNTs with zigzag configuration have a higher elastic modulus than the ones with armchair configuration. On a similar line, Odegard *et al.*[12] proposed equivalent-continuum modeling which serves as a link between computational chemistry and solid mechanics by substituting discrete molecular structures with equivalent-continuum models. It has been shown that this substitution may be accomplished by equating molecular potential energy of a nanostructured material with strain energy of representative truss and continuum models.

Yet other analytical methods include local and nonlocal continuum models. These have negligible computational costs compared to the MD calculations and provide for efficient parametric studies. Peddieson *et al.*[13] used the strain gradient version of a nonlocal continuum model in combination with the theory of an Euler–Bernoulli beam. They used equilibrium to obtain the necessary equations. The investigations showed that nonlocality does not influence the microscale behavior but has a significant effect on the response at the finer nanoscales (CNTs). Sudak[6] also used a Bernoulli beam to investigate the buckling behavior of multiwalled nanotubes. They used a stress gradient model to accommodate small scale effects and also incorporated van der Waals forces between the individually modeled beams. Results showed that small scale effects cannot be neglected. A more sophisticated model for beam buckling was used by Wang *et al.*[14] They implemented a nonlocal continuum model using stress gradient theory on a Timoshenko beam. The governing equations were derived by using the principle of virtual work. By doing this, a more refined model was created that also takes the influence of shear forces into consideration. As expected, the results showed that the buckling load predicted by the Euler–Bernoulli beam model is higher than that predicted by the Timoshenko beam model. Zhang *et al.*[15] used a nonlocal stress gradient model on cylindrical shells to investigate the small scale effects on multiwalled CNTs (MWCNTs). Equilibrium analysis was used to derive the governing equations. With some simplifications, they derived an explicit equation for the axial buckling strain of MWCNTs. It was concluded that nonlocality diminishes the buckling load. Wang *et al.*[16] presented stability analysis using local elastic continuum beam and shell model. They claimed that cylindrical shell-like structure may display two kinds of instability pattern, that is, in one case tube preserves its circular cross section (like shell) and in other case, central axis of tube deforms sideways as a whole (like beam). Thus a different continuum model was used at different stages of the instability. Guduru *et al.*[17] conducted the uniaxial and shell buckling experiments on MWCNT using nanoindentation technique and concluded that theoretically calculated buckling loads are 40%–50% smaller than experimentally measured buckling loads. They attributed this discrepancy to the imperfection in the MWCNTs in the form of sp^3 bonds between the tube walls, which introduce shear coupling between them.

Zhang *et al.*[18] and Lu *et al.*[19] have also investigated the dynamical properties of CNTs using nonlocal theories. Zhang *et al.*[18] showed that for a double walled CNT, the natural frequencies and the associated amplitude of ratios of inner to outer tubes are dependent on the small scale effects, while Lu *et al.*[19] showed that amplitudes of vibration modes decrease when nonlocal effects are increased and concluded that dynamic sensitivity of a NEMS device tends to reduce with size. More recently, Lim *et al.*[20] presented solutions for beam deflection using asymptotic higher order strain gradient nonlocal stress model. However, geometric nonlinearity was not considered during the variational analysis. Wang *et al.*[21] investigated small scale effects on buckling analysis of CNTs using nonlocal stress gradient approach for beam and shell models. Reddy,[22] has provided a comprehensive overview of the use of nonlocal theories for modeling beam bending, vibration, and buckling.

The present paper is concerned with the derivation of the governing equations for buckling of nanotubes modeled as nonlocal one dimensional continua, using both a stress gradient and a strain gradient approach. In the latter case, the variationally consistent sets of boundary conditions are determined. It is shown that, for certain types of boundary conditions, the buckling load exhibits a significant sensitivity to

the nonlocal parameter. Furthermore, the nonlocal models predict buckling loads that are smaller than the corresponding classical counterparts.

II. NONLOCAL CONSTITUTIVE MODELS

Nonlocal continuum field theories are concerned with the physics of material bodies whose behavior at a material point is influenced by the state of all points in the body. The nonlocal theory generalizes the classical field theory in two respects: (1) the energy balance law is considered valid globally (for the entire body) and (2) the state of the body at a material point is described by response functional.[23]

A. Nonlocal elasticity

In the theory of nonlocal elasticity, the stress at a reference point x is considered to be functional of strain field at every point x' in the body. This observation is in accordance with atomic theory of lattice dynamics and phonon dispersion. For homogeneous isotropic bodies, the linear theory leads to a set of integropartial differential equations for the displacement field, which are usually difficult to solve.

For homogeneous and isotropic elastic solids, the linear theory is expressed by the following equation:[24]

$$t_{kl}(x) = \int_V \alpha(|x' - x|, \tau) \, . \, \sigma_{kl}(x') dv(x'), \tag{1}$$

where t_{kl} is the stress tensor at a reference point x in the body at time t. $\sigma_{kl}(x')$ is the macroscopic (classical) stress tensor at x' which is related to linear strain tensor $e_{kl}(x')$ at any point x' in the body at time t with Lame constants, λ and μ.

In Eq. (1), the term $\alpha(|x'-x|, \tau)$ is defined as nonlocal modulus and has the dimension of $(length)^{-3}$. It depends on the characteristic length ratio a/l, where a an is internal characteristic length (e.g., lattice parameter and granular distance) and l is an external characteristic length (e.g., crack length and wavelength.) Thus we can define nonlocal parameter as

$$\tau = e_0 a/l, \tag{2}$$

where e_0 is a constant appropriate to each material.

Using some simplification, the integropartial differential equation can be converted into a partial differential equations. Therefore, Hooke's law can be modified for a uniaxial stress state to give the following constitutive relation:

$$\sigma(x) - (e_0 a)^2 \frac{d^2\sigma(x)}{dx^2} = E\epsilon(x). \tag{3}$$

The constant e_0 is determined from experiments or by matching dispersion curves of plane waves with those of atomic lattice dynamics.

III. STRESS GRADIENT APPROACH

This has been the most common approach used for the analysis of carbon nanotubes using nonlocal theory. For the beam model, the stress gradient approach results in a fourth order differential equation and thus conventional boundary conditions can be used. Using (3), the moment-curvature relation in nondimensionalized form can be modified as

$$M(x) - (e_0 a/L)^2 \frac{d^2M(x)}{dx^2} = -EI\frac{d^2w}{dx^2}. \tag{4}$$

For a beam, the relation between the external applied loads, the internal moment, and internal shear force can be expressed using the following equations:

$$\frac{dV}{dx} = -p(x),$$

$$V = \frac{dM(x)}{dx} + N\frac{dw}{dx}. \tag{5}$$

Using the above equations, the nonlocal deflection curve of an elastic column under constant applied axial compressive load P and distributed lateral load p can be obtained as

$$EI\frac{d^4w}{dx^4} - N\frac{d^2w}{dx^2} - p(x) + (e_0 a)^2\left(\frac{d^2p(x)}{dx^2} + N\frac{d^4w}{dx^4}\right) = 0. \tag{6}$$

Note that N is the internal axial stress resultant and from in-plane equilibrium, $N=-P$, since the in-plane equilibrium equation is $dN/dx=0$. In the limit of vanishing $e_0 a=0$, the above equation reverts to the classical Euler–Bernoulli beam buckling equation.[25]

A. Analytical solution for beam modeled using stress gradient approach

For the buckling analysis, set $p=0$ and nondimensionalize the above equation using L (length of the beam) as a nondimensionalizing parameter. Then, it follows that Eq. (6) can be rewritten as (note, $w=w/L$, $x=x/L$)

$$\frac{d^4w}{dx^4}(1 - (e_0 a/L)^2\pi^2 r) + \pi^2 r\frac{d^2w}{dx^2} = 0,$$

where

$$r = \frac{P}{P_{cr}} = \frac{PL^2}{EI\pi^2}.$$

The general solution to the above differential equation is given by

$$w(x) = C_1 + C_2 x + C_3 \sin(m) + C_4 \cos(m), \tag{7}$$

where $m = (\pi\sqrt{r}x/\sqrt{1-(e_0 a)^2\pi^2 r})$.

Using the appropriate boundary conditions, the above equation can be solved to obtain the critical buckling load. For simply supported boundary conditions, the bending moment M and the beam deflection $w(x)$ vanish at the beam ends. However, the bending moment given by Eq. (4) is a differential equation. Thus, Eq. (4) can be rewritten assuming that $(e_0 a/L)^2 \ll 1$ as

$$M(x) = -EI\left(\frac{d^2w}{dx^2} + (e_0 a/L)^2\frac{d^4w}{dx^4}\right).$$

Similarly, the shear force can be modified to get an expression in terms of displacement gradients, as follows:

$$V(x) = -EI\left(\frac{d^3w}{dx^3} + (e_0a/L)^2\frac{d^5w}{dx^5}\right) - P\frac{dw}{dx}.$$

IV. STRAIN GRADIENT APPROACH

The differential equation for stress shown in Eq. (3) can be solved to determine stress as a function of displacement. Assuming $(e_0a/L)^2 \ll 1$, higher powers of e_0a/L can be neglected and the solution can be simplified to obtain

$$\sigma(x) = E\left(\epsilon(x) + (e_0a)^2\frac{d^2\epsilon(x)}{dx^2}\right), \tag{8}$$

where the usual definitions of strains were used, that is,

$$\epsilon(x) = \frac{du}{dx} + \frac{1}{2}\left(\frac{dw}{dx}\right)^2 - z\frac{d^2w}{dx^2}.$$

The moment-curvature relationship for the strain gradient theory is given by

$$M = -\left(EI\frac{d^2w}{dx^2} + (e_0a)^2EI\frac{d^4w}{dx^4}\right).$$

Using Eq. (5) and the above results, the transverse equilibrium equation for an axially loaded beam using a nonlocal strain gradient theory is obtained as

$$(e_0a)^2EI\frac{d^6w}{dx^6} + EI\frac{d^4w}{dx^4} - N\frac{d^2w}{dx^2} = 0, \tag{9}$$

where N is the axial force in the beam. It is noted that, once again, axial equilibrium dictates that $N=-P$, where P is the applied external axial compression. This equation is similar to that obtained by Peddison *et al.*[13]

A. Analytical solution for beam modeled using strain gradient approach

To find an analytical solution, the equilibrium equation is first normalized as before. Thus, using the length of the beam as the nondimensionalizing parameter, the following sixth order equation is obtained:

$$\frac{d^6w}{dx^6} + \left(\frac{L}{e_0a}\right)^2\frac{d^4w}{dx^4} + \left(\frac{L}{e_0a}\right)^2\pi^2r\frac{d^2w}{dx^2} = 0, \tag{10}$$

where $\pi^2P/P_{\text{crit}} = PL^2/EI = \pi^2r$, and $P=-N$ is the applied axial compression load.

Depending on the ratio of (L/e_0a), this equation exhibits different solutions. One of the solutions is

$$w = C_1 + C_2x + C_3\sin(P) + C_4\cos(P) + C_5\sin(Q) + C_6\cos(Q),$$

with

$$P = \left(\frac{1}{2}\sqrt{\frac{L}{e_0a}}\sqrt{\frac{L}{e_0a} - 2\sqrt{\left(\frac{L}{e_0a}\right)^2 - 4\pi^2r}}\right)x,$$

$$Q = \left(\frac{1}{2}\sqrt{\frac{L}{e_0a}}\sqrt{\frac{L}{e_0a} + 2\sqrt{\left(\frac{L}{e_0a}\right)^2 - 4\pi^2r}}\right)x,$$

if

$$\left(\frac{L}{e_0a}\right)^2 > 4\pi^2r.$$

The other solution is given by

$$w = C_1 + C_2x + C_3e^{-R}\sin S + C_4e^{R}\sin S + C_5e^{-R}\cos S + C_6e^{R}\cos S,$$

with

$$R = \left(\frac{1}{2}\sqrt{2\frac{L}{e_0a}\pi\sqrt{r} - \left(\frac{L}{e_0a}\right)^2}\right)x,$$

$$S = \left(\frac{1}{2}\sqrt{2\frac{L}{e_0a}\pi\sqrt{r} + \left(\frac{L}{e_0a}\right)^2}\right)x,$$

if

$$\left(\frac{L}{e_0a}\right)^2 < 4\pi^2r.$$

The second solution has not been used in the analysis and is only stated for completeness. For the scope of this paper, the parameter that describes the nonlocality has only been varied to such extent $(e_0a/L < 0.1)$ that the first solution to the differential equation is always found to be valid.

B. Strain gradient variational approach

Equation (9) is a sixth order equation and its solution would require additional boundary conditions which cannot be obtained by the direct Newtonian approach. This issue can be settled by using a variational approach.

The potential energy for a beam subjected to external axial force N_0 and lateral load p per unit length in the presence of nonlocal effects is given by

$$\int_V\left(E\frac{\epsilon(x)^2}{2} - (e_0a)^2\frac{E}{2}\left(\frac{d\epsilon(x)}{dx}\right)^2\right)dv - \int_0^L\left(N_0\frac{du}{dx}\right)dx - \int_0^L pw(x)dx. \tag{11}$$

For the buckling analysis, substitute $p=0$. Then by performing a variational process as discussed in Ref. 25, the following equations are obtained (where the subscript NL donates the nonlocal terms and CL the classical terms).

- For variation with respect to $u(x)$:
  - boundary conditions,

$$(e_0a)^2\left(\frac{dN_{CL}}{dx}\right)\left.\frac{d\delta u}{dx}\right|_0^L = 0, \tag{12}$$

$$(N_{\text{NL}} + N_0)\delta u|_0^L = 0. \tag{13}$$

  - governing differential equation,

$$\left(\frac{dN_{\text{NL}}}{dx}\right) = 0, \tag{14}$$

where

TABLE I. Different sets of boundary conditions for a simply supported beam.

BC	SS1	SS2
1,2	$w=0$ at $x=0,1$	$w=0$ at $x=0,1$
3,4	$M_{NL}=0$ at $x=0,1$	M_{NL} at $x=0,1$
5,6	$\frac{d^2w}{dx^2}=0$ at $x=0,1$	$\frac{d^3w}{dx^3}=0$ at $x=0,1$

$$N_{CL} = EA\left(\frac{du}{dx} + \frac{1}{2}\left(\frac{dw}{dx}\right)^2\right)$$

(local axial force inside beam)

$$N_{NL} = N_{CL} + (e_0a)^2\frac{d^2N_{CL}}{dx^2}.$$

- For variation with respect to $w(x)$.
  - boundary conditions,

$$(e_0a)^2\left(EI\frac{d^3w}{dx^3}\right)\left.\frac{d^2\delta w}{dx^2}\right|_0^L = 0, \tag{15}$$

$$\left(EI\frac{d^2w}{dx^2} + (e_0a)^2EI\frac{d^4w}{dx^4}\right)\left.\frac{d\delta w}{dx}\right|_0^L = 0, \tag{16}$$

$$\left(-\left(EI\frac{d^3w}{dx^3} + (e_0a)^2EI\frac{d^5w}{dx^5}\right) + N_{NL}\frac{dw}{dx}\right)d\delta w|_0^L = 0. \tag{17}$$

  - governing differential equation,

$$EI\frac{d^4w}{dx^4} + (e_0a)^2EI\frac{d^6w}{dx^6} - \frac{d}{dx}\left(N_{NL}\frac{dw}{dx}\right) = 0. \tag{18}$$

Since, $dN_{NL}/dx=0$ [using differential equation (14)] and $N_{NL}+N_0=0$ [boundary condition (13)] and $N_{NL}=-N_0$ =const. Substituting this result in the equilibrium equation (18), the earlier derived equation (9) is obtained.

V. RESULTS AND DISCUSSION

Discussion on non-local parameter e_0

The magnitude of the non-local parameter, e_0, determines the nonlocal effect in the analysis. As defined by Eringen,[24] e_0 is a constant appropriate to each material. For example, for a certain class of materials, by comparing the results of lattice dynamics with non-local theory, it was found that,[24] $e_0=0.39$. According the Sudak,[6] values of e_0 need to be determined from experimental results, which for SWCNTs are scarce. On the basis of results presented in,[6] it was concluded that L/a and e_0 be of the same order or one order less to have any significant non-local effect. Zhang *et al.*[16] estimated the value of e_0 by curve fitting the theoretical results obtained using non-local elasticity to those from MM simulations for the critical axial buckling strain of SWCNT. MM results obtained by Sears and Batra,[26] were compared to the obtained for a nanotube modeled as a non-local elastic cylindrical shell using Donell theory and the value of e_0 was approximated as 0.82. Wang *et al.*[17] used the value $0<e_0<7$ for their analysis, which are much higher than values predicted earlier. Zhang *et al.*[7] determined the values of e_0 for different chiral angles, (m,n), by curve fitting the results obtained by MD simulations and non-local analysis results obtained using their Donell shell model. Values obtained varied from a minimum of 0.546 for a (15,4) chiral shell to a maximum of 1.043 for a (11,9) chiral shell. Thus, it is seen that accurate values of e_0 are yet to be determined. In the present analysis, the non-dimensional term e_0a/l is kept variable and its effect on the predicted buckling response is de-

TABLE II. Different sets of boundary conditions for a clamped beam.

BC	CC1	CC2
1,2	$w=0$ at $x=0$ and $x=1$	$w=0$ at $x=0$ and $x=1$
3,4	$\frac{dw}{dx}$ at $x=0$ and $x=1$	$\frac{dw}{dx}$ at $x=0$ and $x=1$
5,6	$\frac{d^3w}{dx^3}=0$ at $x=0$ and $x=1$	$\frac{d^2w}{dx^2}=0$ at $x=0$ and $x=1$

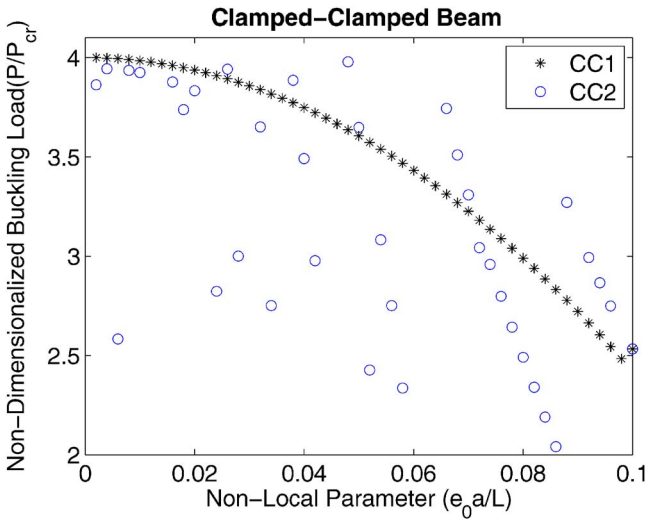

FIG. 3. (Color online) Clamped at both ends.

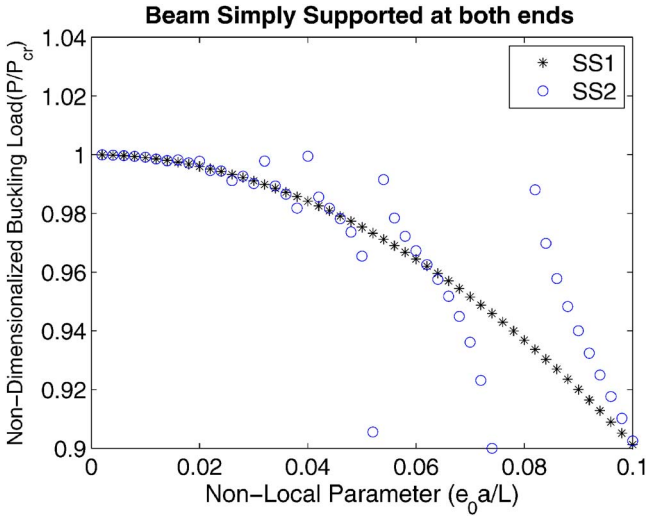

FIG. 4. (Color online) Simply supported at both ends.

TABLE III. Set of boundary conditions for clamped simply supported (CS) beam.

BC	CS1	CS2
5	$\frac{d^3w}{dx^3}=0$ at $x=0$	$\frac{d^2w}{dx^2}=0$ at $x=0$
6	$\frac{d^2w}{dx^2}=0$ at $x=1$	$\frac{d^2w}{dx^2}=0$ at $x=1$
BC	CS3	CS4
5	$\frac{d^3w}{dx^3}=0$ at $x=0$	$\frac{d^2w}{dx^2}=0$ at $x=0$
6	$\frac{d^3w}{dx^3}=0$ at $x=1$	$\frac{d^3w}{dx^3}=0$ at $x=1$

termined. Furthermore, the manner in which e_0a/l enters the boundary conditions are derived in a variationally consistent manner.

B. To determine the effects of different boundary conditions

Using the variational analysis, additional sets of variationally consistent boundary conditions are obtained. As shown in Eq. (15), the additional boundary condition implies that either the second derivative of displacement is zero or the third derivative of displacement is zero. To simplify the equations, let us define a nonlocal moment (M_{NL}) and a corresponding nonlocal shear force (V_{NL}), as shown in Eq. (19).

$$M_{NL} = -EI\left(\frac{d^2w}{dx^2} + (e_0a)^2\frac{d^4w}{dx^4}\right),$$

$$V_{NL} = -EI\left(\frac{d^3w}{dx^3} + (e_0a)^2\frac{d^5w}{dx^5}\right) + N_{NL}\frac{dw}{dx}. \quad (19)$$

In order to investigate the effects of these variationally consistent sets of different boundary conditions, the buckling behavior of a beam "simply supported" at both ends and a beam "clamped" at both ends was considered. Table I shows two different sets of boundary condition for a beam simply supported at both ends labeled as SS1 and SS2.

Similarly Table II shows two sets of boundary conditions for a beam clamped at both ends labeled as CC1 and CC2.

Figure 3 shows the variation of the critical buckling load ratio with nonlocal parameter e_0a/L for a beam clamped at both ends. The dependence obtained using $d^3w/dx^3=0$ (CC1) shows a smooth variation whereas the dependence obtained using $d^2w/dx^2=0$ (CC2) does not show such a smooth variation, which is unexpected. Thus it appears from the results obtained above that the CC1 boundary condition gives results that show a monotonic dependence of buckling load on the nonlocal parameter.

A similar analysis was done for a beam simply supported at both ends (Fig. 4). In this case, the dependence obtained using $d^2w/dx^2=0$ (SS1) shows a smooth variation, whereas the dependence obtained using $d^3w/dx^3=0$ (SS2) does not show such a smooth variation. Again, therefore, it appears that for a simply supported beam, the SS1 boundary conditions give results that show a monotonic dependence of buckling load on the nonlocal parameter.

In order to further verify the results obtained above, a beam simply supported at one end ($x=1$) and clamped at the other end ($x=0$) was considered. Here, four different sets of boundary conditions were considered, as shown in Table III. As shown in Figure 5, only the CS1 set of boundary conditions provides a smooth variation in buckling load with nonlocal parameter.

A careful examination of the results presented here now shows that using $d^2w/dx^2=0$ as the additional boundary condition for a simply supported edge and using $d^3w/dx^3=0$ as the additional boundary condition for a clamped edge pro-

TABLE IV. Cantilevered beam (CF).

BC	CF1	CF2
1	$M_{NL}=0$	$M_{NL}=0$
2	$V_{NL}=0$	$V_{NL}=0$
3	$\frac{d^2w}{dx^2}=0$	$\frac{d^3w}{dx^3}=0$

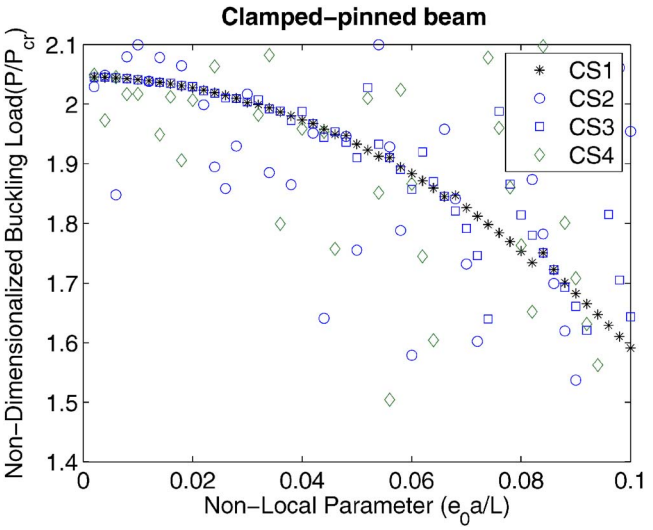

FIG. 5. (Color online) Clamped-pinned beam.

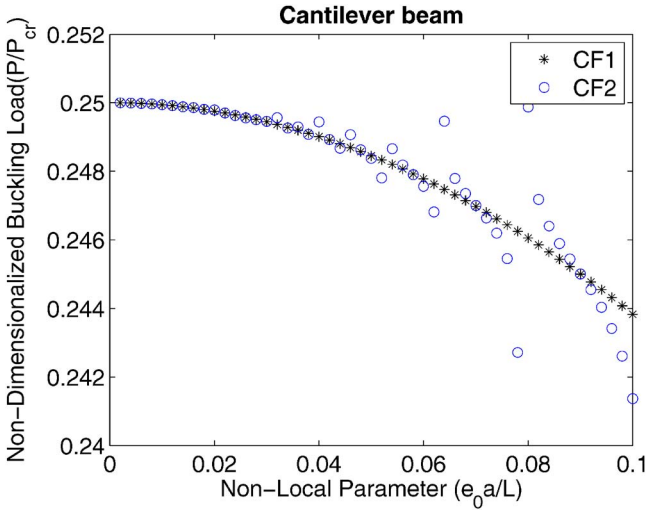

FIG. 6. (Color online) Cantilevered beam.

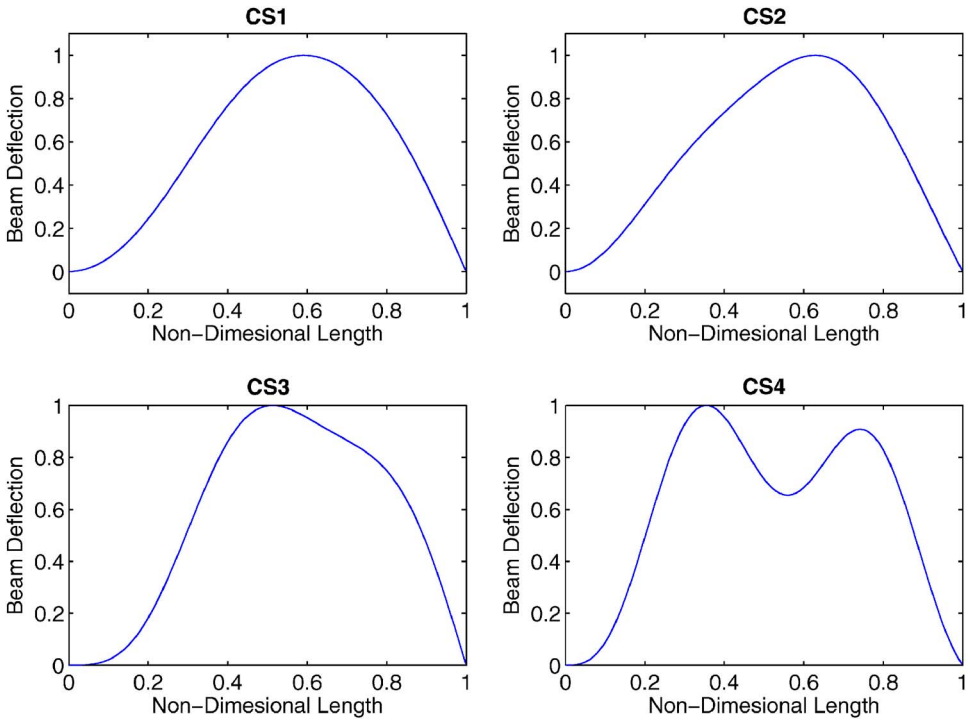

FIG. 7. (Color online) Shape function for clamped simply supported beam at $a_0 a/L=0.07$.

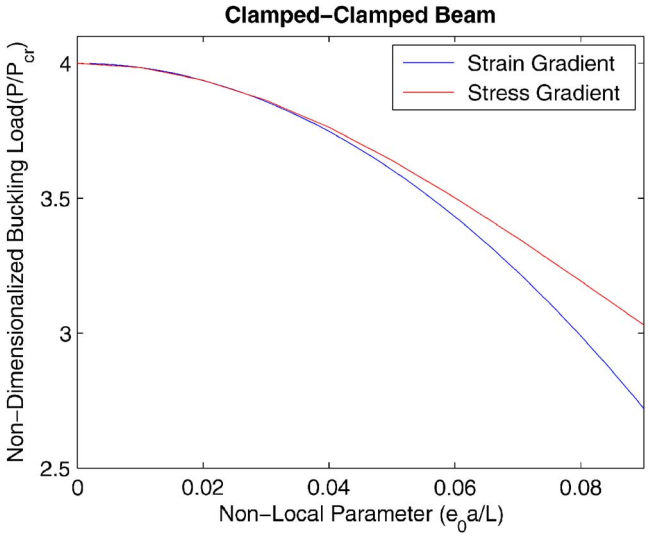

FIG. 8. (Color online) Clamped-clamped beam.

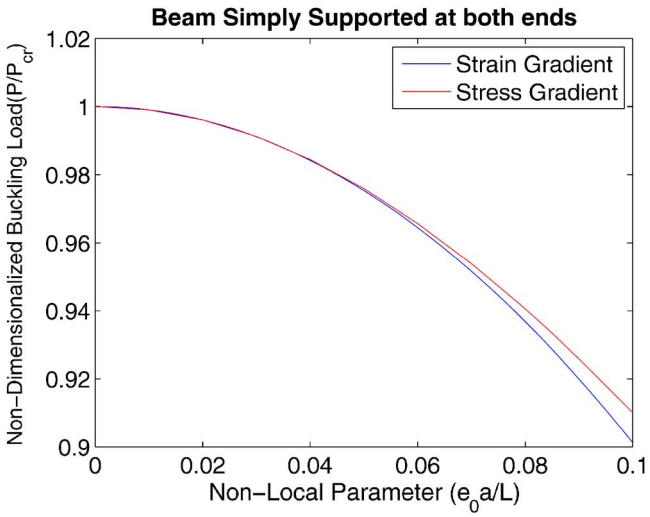

FIG. 9. (Color online) Simply supported beam.

vide a monotonic dependence of buckling load on nonlocal parameter. In order to establish boundary conditions for a free end, the buckling problem for a cantilevered nonlocal beam was considered. Table IV shows two different sets of boundary conditions for free end.

Figure 6 shows the variation obtained using two sets of boundary conditions for a cantilevered beam. From this figure, it appears that the CF1 set of boundary conditions provides the requisite variation in buckling load with nonlocal parameter.

To further consolidate these findings with respect to the results being physically meaningful, the shape of the buckled beams corresponding to the calculated buckling loads was examined. Physical meaningfulness is defined here on the basis of the manner in which the buckling load shows dependence on nonlocal parameter *and* on the resulting "smoothness" of the buckled mode shape. Figure 7 shows the buckled mode shape for a clamped simply supported beam correspoding to different sets of boundary conditions. Only the buckled mode shape corresponding to CS1 shows a smooth variation in beam slope, while in other cases "wiggly" beam deflections are observed. Similar wiggly buckled mode shapes were obtained for clamped-clamped, simply supported, and cantilevered beams with different choice of boundary conditions; however, in each case these modes corresponded to those instances in which the buckling load did not show a monotonic dependence on nonlocal parameter.

C. Comparison with stress gradient approach

Results obtained using the strain gradient variational approach were compared to the analytical solution obtained using the stress gradient approach discussed in Sec. III as shown in Figs. 8 and 9. For each comparison, the stress gradient approach suggests a higher buckling load than the strain gradient approach. Thus, the strain gradient nonlocal

model provides a lower bound on the buckling load of CNTs modeled in the manner described in this paper.

VI. CONCLUSIONS

The buckling behavior of CNTs, incorporating a constitutive law that includes a length scale, has been analyzed using a direct Newtonian approach and a variational approach. The latter approach provides the governing field equations and the variationally consistent sets of boundary conditions. Incorporation of small length scale effects are found to significantly affect the buckling behavior. Depending on the material constant e_0a/L, the buckling load varies monotonically from the classical value to values that are lower. As the nonlocal characteristic parameter e_0a/L increases, a decrease in buckling load is observed and this effect has been quantified for different boundary conditions. Careful experiments are required to determine the material constant e_0, and it appears that the results presented here can form the basis for an experimental program to determine this constant. The variational approach that has been presented yields an extra pair of variationally consistent boundary conditions. Nevertheless, only one of the two choices appears to provide physically meaningful results.

[1]S. Iijima, Nature (London) **56**, 354 (1991).
[2]E. T. Thostensona, Z. Renb, and T.-W. Choua, Compos. Sci. Technol. **61**, 1899 (2001).
[3]R. H. Baughman, A. A. Zakhidov, and W. A. de Heer, Science **297**, 787 (2002).
[4]S. S. Wong, E. Joselevich, A. T. Woolley, C. L. Cheung, and C. M. Lieber, Nature (London) **394**, 52 (1998).
[5]D. Keller, Nature (London) **384**, 111 (1996).
[6]L. J. Sudak, J. Appl. Phys. **94**, 7281 (2003).
[7]Y. Y. Zhang, V. B. C. Tan, and C. M. Wang, J. Appl. Phys. **100**, 074304 (2006).
[8]D. Frenkel and B. Smit, *Understanding Molecular Simulation: From Algorithms to Applications* (Academic, San Diego, 2002).
[9]J. M. Haile, *Molecular Dynamics Simulation: Elementary Methods* (Wiley, New York, 1997).
[10]B. Yakobson, C. J. Brabec, and J. Bernholc, Phys. Rev. Lett. **76**, 2511 (1996).
[11]C. Li and T.-W. Chou, Int. J. Solids Struct. **40**, 2487 (2003).
[12]G. M. Odegard, T. S. Gates, L. M. Nicholson, and K. E. Wise, Compos. Sci. Technol. **62**, 1869 (2002).
[13]J. Peddieson, G. R. Buchanan, and R. P. McNitt, Int. J. Eng. Sci. **41**, 305 (2003).
[14]C. M. Wang, Y. Y. Zhang, S. S. Ramesh, and S. Kitipornchai, J. Appl. Phys. **39**, 3904 (2006).
[15]Y. Q. Zhang, G. R. Liu, and J. S. Wang, Phys. Rev. B **70**, 205430 (2004).
[16]Q. Wang and V. Varadan, Smart Mater. Struct. **14**, 281 (2005).
[17]P. R. Guduru and Z. Xia, Exp. Mech. **47**, 153 (2007).
[18]Y. Q. Zhang, G. R. Liu, and X. Y. Xie, Phys. Rev. B **71**, 195404 (2005).
[19]P. Lu, H. P. Lee, C. Lu, and P. Q. Zhang, J. Appl. Phys. **99**, 073510 (2006).
[20]C. W. Lim and C. M. Wang, J. Appl. Phys. **101**, 054312 (2007).
[21]Q. Wang, V. K. Varadan, and S. T. Quek, Phys. Lett. A **357**, 130 (2006).
[22]J. Reddy, Int. J. Eng. Sci. **45**, 288 (2007).
[23]A. C. Eringen, *Non Local Continuum Field Theories* (Springer, New York, 2002).
[24]A. C. Eringen, J. Appl. Phys. **54**, 4703 (1983).
[25]D. O. Brush and B. O. Almroth, *Buckling of Bars, Plates and Shells* (McGraw-Hill Education, New York, 1975).
[26]A. Sears and R. C. Batra, Phys. Rev. B **69**, 235406 (2004).